Ab initio calculations of elastic properties of bcc Fe-Mg and Fe-Cr random alloys

Hualei Zhang,[1] Börje Johansson,[1,2,3] and Levente Vitos[1,3,4]
[1]*Department of Materials Science and Engineering, Applied Materials Physics, Royal Institute of Technology, SE-10044 Stockholm, Sweden*
[2]*School of Physics and Optoelectronic Technology and College of Advanced Science and Technology, Dalian University of Technology, Dalian 116024, China*
[3]*Department of Physics and Materials Science, Division of Materials Theory, Uppsala University, SE-75121 Uppsala, Box 530, Sweden*
[4]*Research Institute for Solid State Physics and Optics, P.O. Box 49, H-1525 Budapest, Hungary*
(Received 16 February 2009; published 4 June 2009)

Using the *ab initio* exact muffin-tin orbitals method in combination with the coherent-potential approximation, we have calculated the elastic parameters of ferromagnetic $Fe_{1-m}Mg_m$ $(0 \leq m \leq 0.1)$ and $Fe_{1-c}Cr_c$ $(0 \leq c \leq 0.2)$ random alloys in the body-centered cubic (bcc) crystallographic phase. Results obtained for $Fe_{1-c}Cr_c$ demonstrate that the employed theoretical approach accurately describes the experimentally observed composition dependence of the polycrystalline elastic moduli of Fe-rich alloys encompassing maximum ~10% Cr. The elastic parameters of Fe-Cr alloys are found to exhibit anomalous composition dependence around 5% Cr. The immiscibility between Fe and Mg at ambient conditions is well reproduced by the present theory. The calculated lattice parameter for the Fe-Mg regular solid solution increases by ~1.95% when 10% Mg is introduced in Fe, which corresponds approximately to 11% decrease in the average alloy density, in perfect agreement with the experimental finding. At the same time, we find that all of the elastic parameters of bcc Fe-Mg alloys decrease almost linearly with increasing Mg content. The present results show a much stronger alloying effect for Mg on the elastic properties of α-Fe than that for Cr. Our results call for further experimental studies on the mechanical properties of the Fe-Mg system.

DOI: 10.1103/PhysRevB.79.224201 PACS number(s): 71.15.Nc, 71.20.Be, 62.20.D−, 81.05.Zx

I. INTRODUCTION

According to the common phase diagrams, iron and magnesium are almost immiscible at ambient pressure.[1] In the liquid phase, the solubility of Mg in Fe is on the order of 0.025 atomic percent (at. %). The maximum solid solubility of Fe in Mg is 0.00041 at. % and the Fe content in Mg at the eutectic point is less than 0.008 at. %.[2] Below 1273 K the solubility of Mg in α-Fe is below the detection limit and about 0.25 at. % Mg can be solved in δ-Fe at the monotectic temperature. The immiscibility of Fe and Mg at ambient conditions is in line with the well-known Hume-Rothery rules, according to which more than 15% atomic size difference between alloy constituents hinders solid solution formation.[3]

In spite of the negligible solubility of Mg in Fe, several Fe-rich metastable Fe-Mg solid solutions have been synthesized. According to the pioneering work by Hightower *et al.*,[4] mechanical alloying produced Fe-Mg substitutional solid solutions with up to 20 at. % Mg and having the body-centered-cubic (bcc) crystallographic phase of α-Fe. Later, using the similar alloying procedure, Dorofeev *et al.*[5–7] found that about 5–7 at. % Mg in α-Fe forms supersaturated solid solution. These authors suggested that the driving force for the formation of Fe-Mg solid solutions is associated with the excess energy of coherent interfaces in the Fe-Mg nanocomposite, which facilitates incorporation of Mg into α-Fe. Indeed, based on semiempirical thermodynamic calculations, Yelsukov *et al.*[7] obtained 6 kJ/mol for the enthalpy of formation for $Fe_{0.93}Mg_{0.07}$, compared to 20 kJ/mol calculated for the corresponding Fe-Mg nanocomposites.

In addition to the mechanical alloying techniques, pressure was also found to facilitate the solid solution formation between Fe and Mg. Dubrovinskaia *et al.*[8] reported that at pressures around 20 GPa and temperatures up to 2273 K, the solubility of Mg in bcc Fe was increased to 4 at. %. They found that the lattice parameter of the bcc Fe-Mg alloy increased approximately by 0.6% per at. % Mg. Furthermore, recent theoretical simulations in combination with experimental measurements demonstrated that at the megabar pressure range more than 10 at. % Mg could be dissolved in liquid Fe, which then could be quenched to ambient conditions.[9] The mechanism behind the high-pressure alloying is the much larger compressibility of Mg compared to that of Fe.

Most of the theoretical and experimental investigations of the Fe-Mg solid solutions so far focused on the phase diagram, crystallographic structure, nanostructure, grain boundaries, and segregation. However, much less is known about the mechanical properties of Fe-rich Fe-Mg alloys. Here we present a systematic first-principles study of the effect of Mg on the elastic properties of ferromagnetic bcc Fe-Mg alloys. We calculate the single crystal and polycrystalline elastic parameters by using the all-electron exact muffin-tin orbitals (EMTO) method[10–12] in combination with the coherent-potential approximation (CPA).[13–16] Since at ambient conditions the Fe-rich Fe-Mg alloys were found to adopt the ferromagnetic bcc structure,[4,5,9] all calculations are performed for this magnetic and crystallographic phase. Using Mössbauer spectroscopy, Hightower *et al.*[4] found that bcc Fe-Mg alloys encompassing ~18 at. % Mg possess large chemical heterogeneities. According to that study only few Fe atoms have Mg atoms as first-nearest neighbors and the Mg atoms cluster into Fe-depleted zones on the bcc lattice. On the other hand, Dorofeev *et al.*[5,7] determined the effect of nearest-neighbor and next-nearest-neighbor Mg atom on the hyper-

fine magnetic field of Fe nuclei in Fe-Mg alloys containing 5–7 at. % Mg. Moreover, the $Fe_{0.96}Mg_{0.04}$ synthesized by Dubrovinskaia *et al.*[8] at high temperature and moderate pressures was reported to be homogeneous. It is also noticeable the excellent agreement obtained between the experimental and theoretical equation of states for $Fe_{0.96}Mg_{0.04}$, the latter obtained for completely random alloy.[9] These findings indicate that clustering of Mg atoms is less significant in Fe-rich alloys. Because of that, we limit the present study to $Fe_{1-m}Mg_m$ alloys with $0 \leq m \leq 0.1$ and assume random distributions of the Mg atoms on the parent lattice.

In order to assess the accuracy of our theoretical approach, first we carry out a comprehensive study of the elastic properties of Fe and Fe-rich Fe-Cr alloys, for which a vast number of experimental[17–20] and theoretical[21–24] data are available. This study is also of fundamental interest because no *ab initio* theoretical investigation of the elastic properties of Fe-rich Fe-Cr alloys has been presented so far. The Fe-Cr alloys, except the high-temperature Fe-rich γ phase and the σ phase observed around equimolar concentrations, adopt the bcc structure.[25] The present calculations are performed for random $Fe_{1-c}Cr_c$ alloys with $0 \leq c \leq 0.2$. At normal conditions, these bcc alloys are ferromagnetic with Curie temperatures around 900–1050 K.[25] For $c \lesssim 0.1$ and $T \gtrsim 600$ K, the Fe-Cr system is fully miscible, whereas the nucleation or spinodal (α') decomposition-driven clustering occurs at higher Cr concentrations.[26,27] Nevertheless, it has been shown[28,29] that the energetics of Fe-Cr alloys with $\lesssim 20$ at. % Cr are well described using the substitutional disordered ferromagnetic bcc phase employed in the present study.

The paper is divided in two main sections. The theoretical tool is presented in Sec. II. Here we give a brief overview of the electronic structure method and the most important details of the numerical calculations. The results are presented and discussed in Sec. III. After we make a comparison between the present and former theoretical and experimental elastic constants for Fe and Fe-Cr alloys, we put forward our theoretical predictions obtained for the ferromagnetic Fe-Mg solid solution.

II. COMPUTATIONAL METHOD

A. Total energy calculations

The present calculations are based on density functional theory (DFT) (Ref. 30) formulated within the Perdew-Burke-Ernzerhof generalized gradient approximation[31] for the exchange-correlation functional. The Kohn-Sham equations[32] were solved using the exact muffin-tin orbitals method.[10–12] The substitutional disorder was treated within the coherent-potential approximation.[13–16] From the self-consistent charge density the total energy was calculated using the full charge-density technique.[33]

The EMTO method is an improved screened Korringa-Kohn-Rostoker method,[10] where the full potential is represented by overlapping muffin-tin potential spheres. By using overlapping spheres one describes more accurately the exact crystal potential, when compared to the conventional muffin-tin or nonoverlapping methods.[12,34] Further details about the EMTO method and its self-consistent implementation can be found in Refs. 10–12, 15, and 16. The EMTO approach ensures the accuracy needed for the calculations of anisotropic lattice distortions in random alloys. It has been applied successfully in the *ab initio* study of the thermophysical properties of random Fe-based alloys,[9,28,35–38] simple- and transition-metal alloys,[12,39–43] and oxide solid solutions.[44–47]

B. Numerical details

The elastic properties of single crystals are described by the elements C_{ij} of the elasticity tensor. There are three independent elastic constants for a cubic lattice: C_{11}, C_{12}, and C_{44}. They are connected to the tetragonal shear-modulus $C'=(C_{11}-C_{12})/2$ and bulk-modulus $B=(C_{11}+2C_{12})/3$. Dynamical (mechanical) stability requires that[48] $C_{44}>0$, $C'>0$ and $B>0$.

In the present study, the cubic elastic constants of the random ferromagnetic bcc $Fe_{1-c}Cr_c$ $(0 \leq c \leq 0.2)$ and $Fe_{1-m}Mg_m$ $(0 \leq m \leq 0.1)$ were calculated as a function of the chemical composition. At each concentration the theoretical equilibrium volume and the bulk modulus were derived from an exponential Morse-type function[49] fitted to the *ab initio* total energies of bcc structures calculated for seven different atomic volumes. In order to obtain the two cubic shear-moduli C' and C_{44}, we used volume-conserving orthorhombic and monoclinic deformations as described, e.g., in Ref. 50.

From the single-crystal elastic constants we obtained the polycrystalline shear modulus (G) according to the Hill averaging method $G=(G_V+G_R)/2$,[51] where the Reuss and Voigt bounds[16] are

$$G_R = 5(C_{11}-C_{12})C_{44}(4C_{44}+3C_{11}-3C_{12})^{-1},$$

and

$$G_V = (C_{11}-C_{12}+3C_{44})/5. \quad (1)$$

For cubic solids, the polycrystalline bulk modulus is equivalent with the single-crystal bulk modulus, and Young's modulus (E) and the Poisson ratio (ν) are connected to B and G by the relations $E=9BG/(3B+G)$ and $\nu=(3B-2G)/(6B+2G)$. Finally, the polycrystalline elastic Debye temperature (Θ) was calculated from the longitudinal and transversal sound velocities obtained from B, G and the average alloy density (see, e.g., Ref. 50).

In the present electronic-structure and total-energy calculations, the one-electron equations were solved within the scalar-relativistic and soft-core approximations. The Green function was calculated for 16 complex energy points distributed exponentially on a semicircular contour. In the basis set we included s, p, d and f orbitals ($l_{\max}=4$), and the one-center expansion of the full-charge density was truncated at $l^h_{\max}=8$.[16] To obtain the accuracy needed for the calculation of elastic constants we used about 20 000–25 000 uniformly distributed k points in the irreducible wedge of the orthorhombic and monoclinic Brillouin zones. The electrostatic correction to the single-site coherent-potential approximation was described using the original screened impurity model[52] with a screening parameter of 0.6. The radii of the overlap-

ping muffin-tin spheres of Fe, Mg, and Cr were chosen to be equal to the average atomic sphere radius.

III. RESULTS

A. Elastic properties of ferromagnetic bcc Fe

In order to assess the accuracy and reliability of our theoretical tool for pure Fe, in Tables I and II we compare the present equilibrium lattice parameter, single-crystal elastic constants, and polycrystalline elastic moduli for ferromagnetic bcc Fe with former theoretical results and experimental data.

For ferromagnetic bcc Fe, the present theoretical lattice parameter (a) agrees with that calculated using the full-potential linear augmented plane wave (FLAPW) and projector augmented wave (PAW) methods.[21,23] The ~1% deviation between these theoretical values and the experimental lattice parameters[17,20] may be ascribed to the employed generalized gradient approximation,[31] which is known to underestimate the equilibrium volume of magnetic $3d$ metals.[16,54] A similar deviation is obtained for Cr, for which the present theoretical lattice constant is 2.85 Å compared to the measured value of 2.88 Å.[55] At ambient conditions, elemental Cr has an incommensurable antiferromagnetic state, which we approximate by the commensurable antiferromagnetic B2 structure.[56,57]

In Table I, we list four sets of single-crystal elastic constants obtained from four different theoretical studies, all of them employing the generalized gradient approximation for the density functional. Taking the error bar associated with such calculation to be the difference between these four independent full-potential results, we can conclude that the present method gives accurate results for the elastic properties of ferromagnetic Fe. On the other hand, when compared to the experimental data,[17,20] we find that all theoretical approaches overestimate C_{11} and C' but give accurate values for C_{12} and C_{44}. Repeating the EMTO calculation for C' at the experimental volume, we obtain $C'=64.4$ GPa, which demonstrates that the volume effect can account for about 50% of the EMTO error for C'. At the same time, from the measured C_{ij} values for 4.2 and 300 K (Table I) one can see that it is very unlikely that the remaining deviations between theory and experiment to be connected with temperature effects. We speculate that the error in C' has a complex electronic structure and magnetic origin, which is not captured by the present density-functional approximation.

TABLE I. Theoretical and experimental equilibrium lattice parameter (a in Å) and single-crystal elastic constants (in GPa) for ferromagnetic bcc Fe. The quoted theoretical methods are FLAPW: all-electron full-potential linear augmented plane wave (Ref. 21); PP: ultrasoft pseudopotentials (Ref. 22); PAW: projector augmented wave (Ref. 23) and FPLMTO: full-potential linear muffin-tin orbitals (Ref. 24). In the PP and PAW calculations an earlier version of the generalized gradient approximation (Ref. 53) was used. The temperatures for the experimental data (Refs. 17 and 20) are indicated.

	Method	a	C_{11}	C_{12}	C'	C_{44}
Theory	EMTO	2.84	297.8	141.9	77.9	106.7
	FLAPW[a]	2.84	279	140	69	99
	PP[b]	2.83	289	118	85.5	115
	PAW[c]	2.84	271	145	63	101
	FPLMTO[d]	2.81	297	148	74.5	123
Expt.	298 K[e]	2.87	232	136	48	117
	4.2 K[f]	2.87	243.1	138.1	52.5	121.9
	300 K[f]		233.1	135.4	48.3	117.8

[a]Reference 21.
[b]Reference 22.
[c]Reference 23.
[d]Reference 24.
[e]Reference 20.
[f]Reference 17.

TABLE II. Theoretical and experimental polycrystalline elastic constants (in GPa) for ferromagnetic bcc Fe. For notations see caption of Table I. The temperatures for the experimental data (Refs. 17 and 20) are indicated. The theoretical results were derived from the single-crystal data (Table I) using the Hill averaging method (Ref. 51).

	Method	B	G	B/G	E	ν
Theory	EMTO	193.9	94.1	2.06	243.0	0.291
	FLAPW[a]	186	85.9	2.17	223.4	0.300
	PP[b]	175	102	1.72	256.2	0.256
	PAW[c]	187	84	2.23	219.2	0.305
	FPLMTO[d]	201	103	1.95	263.9	0.281
Expt.	298 K[e]	168	81.8	2.05	211.4	0.290
	4.2 K[f]	173.1	87.5	1.98	224.7	0.284
	300 K[f]	167.9	83.4	2.01	214.6	0.287
	298 K[g]	166	80.7	2.06	208.2	0.291
	298 K[h]	168.2	83.7	2.01	215.4	0.287

[a]Reference 21.
[b]Reference 22.
[c]Reference 23.
[d]Reference 24.
[e]Reference 20.
[f]Reference 17.
[g]Reference 18.
[h]Reference 19.

All theoretical polycrystalline elastic moduli for α-Fe, listed in Table II, were obtained using the Hill averaging method described in Sec. II. The general agreement between the five sets of theoretical polycrystalline data is good. The mean deviation between the EMTO values for B, G, E, and ν and the experimental data at 4.2 K (Ref. 17) is around 7%, which is typical for what has been obtained for the transition metals in conjunction with the present density-functional approximation.[16,58] In particular, our approach is found to give B/G and ν for bcc Fe in excellent agreement with experiment.

B. Elastic properties of Fe-Cr alloys

In this section, we investigate the composition dependence of the elastic constants of ferromagnetic bcc $Fe_{1-c}Cr_c$

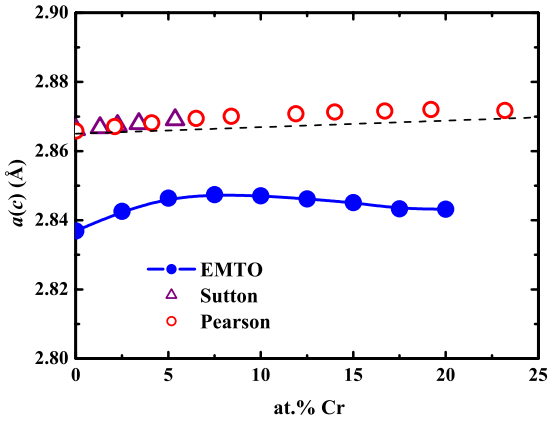

FIG. 1. (Color online) Theoretical (EMTO) and experimental lattice parameter of ferromagnetic bcc Fe-Cr alloys as a function of Cr concentration. The experimental data are from Ref. 59 (Sutton) and Ref. 60 (Pearson). The dashed line is obtained from Vegard's rule.

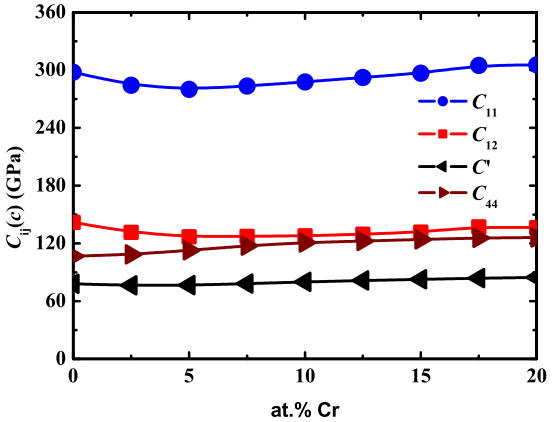

FIG. 2. (Color online) Theoretical (EMTO) single-crystal elastic constants of ferromagnetic bcc $Fe_{1-c}Cr_c$ random alloys as a function of Cr concentration.

$(0 \le c \le 0.2)$ random alloys. This system has been selected because of the following reasons. First, there are experimental polycrystalline elastic moduli available for Fe-Cr alloys for Cr content up to ~10 at. %, and thus this system can be used to establish the accuracy of the EMTO method for the composition dependence of the elastic constants in Fe-rich bcc alloys. Second, no *ab initio* theoretical study of the elastic properties of Fe-rich Fe-Cr alloys has been reported so far in spite of the fact that these alloys constitute the basis for stainless steels.

For each Cr concentration c, the elastic constants were calculated at the corresponding theoretical equilibrium lattice parameter $a(c)$. The composition dependence of $a(c)$ is shown in Fig. 1 along with the experimental data.[59,60] Since the lattice constant of bcc Fe is by ~0.019 Å smaller than that of B2 Cr, based on Vegard's rule we would predict a linear $a(c)$ with slope of $\Delta a(c)/\Delta c \sim 0.2 \times 10^{-3}$ Å per at. % Cr. However, both the experimental and the theoretical lattice parameters deviate from this simple linear trend. The EMTO lattice parameter reaches a maximum value between 7.5 and 10 at. % Cr and remains above the lattice parameter of pure Fe for all concentrations considered here. Using the theoretical values below $c=0.1$, for the slope of $a(c)$ we get $\sim 1.7 \times 10^{-3}$ Å per at. % Cr. This slope is larger than the average experimental value of $\sim 0.5 \times 10^{-3}$ Å per at. % Cr calculated below 10 at. % Cr,[60] but is in perfect agreement with the former *ab initio* calculation based on special quasirandom structures.[29]

In Fig. 2 and Table III, we display the present theoretical single-crystal elastic constants $C_{ij}(c)$ for ferromagnetic bcc $Fe_{1-c}Cr_c$ as a function of Cr concentration for $0 \le c \le 0.2$. We find that $C_{11}(c)$ and $C_{12}(c)$ have local minima around 5 at. % Cr, and these minimal values are by 6% and 10.6% smaller than those corresponding to pure Fe. $C'(c)$ exhibits a somewhat less pronounced minimum at 2.5 at. % Cr. For Cr contents close to 20 at. %, the calculated $C_{11}(c)$, $C'(c)$, and $C_{44}(c)$ are ~2.5, ~8.5, and 18.0%, respectively, lager than those of pure Fe. At the same time, for $c=0.2$, $C_{12}(c)$ is about ~4% smaller than that of bcc Fe.

It is instructive to compare the calculated alloying effects on the elastic constants of Fe-rich Fe-Cr alloys with those estimated from the rule of mixing based on the experimental data for Fe and Cr. Starting from the experimental elastic constants of Fe ($C_{11}=243.1$ GPa, $C_{12}=138.1$ GPa, and $C_{44}=121.9$) (Ref. 61) and Cr ($C_{11}=391.0$ GPa, $C_{12}=89.6$ GPa, and $C_{44}=103.2$ GPa),[61] a linear rule of mixing predicts the following slopes: $\Delta C_{11}(c)/\Delta c \sim 1.5$ GPa, $\Delta C_{12}(c)/\Delta c \sim -0.5$ GPa, and $\Delta C_{44}(c)/\Delta c \sim -0.2$ GPa per at. % Cr. Using the present results for $c \le 0.05$ for the average theoretical slopes we obtain $\Delta C_{11}(c)/\Delta c \sim -4.5$ GPa, $\Delta C_{12}(c)/\Delta c \sim -3.6$ GPa, and $\Delta C_{44}(c)/\Delta c \sim 1.0$ GPa per at. % Cr. Extending the averaging to all compositions below 20 at. % Cr (Table III) gives $\Delta C_{12}(c)/\Delta c \sim -1.6$ GPa per at. % Cr, which is in qualitative agreement with the slope estimated from the rule of mixing. However, even for this large concentration interval, $\Delta C_{11}(c)/\Delta c$ remains negative and $\Delta C_{44}(c)/\Delta c$ positive, which is in sharp contradiction with the rule of mixing. Therefore, in Fe-rich alloys the simple rule of mixing fails to describe the actual trends of $C_{11}(c)$ and $C_{44}(c)$.

Since no experimental single-crystal elastic constants are available for Fe-Cr alloy, we use the measured polycrystalline data[18] to assess the accuracy of our method. The present

TABLE III. Theoretical (EMTO) lattice parameter (in Å) and single-crystal elastic constants (in GPa) for the ferromagnetic bcc $Fe_{1-c}Cr_c$ $(0 \le c \le 0.2)$ random alloys.

c	$a(c)$	$C_{11}(c)$	$C_{12}(c)$	$C'(c)$	$C_{44}(c)$
0	2.8369	297.84	141.89	77.97	106.73
0.025	2.8426	284.17	131.51	76.33	108.56
0.05	2.8464	279.96	126.87	76.54	112.83
0.075	2.8474	283.52	127.19	78.16	117.51
0.10	2.8471	287.75	127.92	79.91	120.71
0.125	2.8462	292.32	129.54	81.39	122.42
0.15	2.8451	296.81	131.65	82.58	124.06
0.175	2.8433	304.95	137.18	83.89	125.58
0.20	2.8432	305.54	136.28	84.63	125.97

TABLE IV. Theoretical polycrystalline elastic constants (in GPa), Poisson' ratio (ν), and Debye temperature (Θ, in K) for the ferromagnetic bcc $Fe_{1-c}Cr_c$ ($0 \leq c \leq 0.2$) random alloys as a function of Cr content.

c	$B(c)$	$G(c)$	$B/G(c)$	$E(c)$	$\nu(c)$	$\Theta(c)$
0	193.9	94.12	2.0598	243.03	0.291	427.41
0.025	182.4	94.27	1.9349	241.25	0.280	426.28
0.05	177.9	96.58	1.842	245.34	0.270	430.40
0.075	179.3	99.79	1.7967	252.53	0.265	437.08
0.10	181.2	102.32	1.7709	258.33	0.262	442.47
0.125	183.8	103.94	1.7683	262.37	0.262	446.08
0.15	186.7	105.39	1.7715	266.09	0.262	449.37
0.175	193.1	106.83	1.8075	270.59	0.266	452.94
0.20	192.7	107.41	1.7941	271.73	0.265	454.11

theoretical polycrystalline elastic parameters for ferromagnetic bcc $Fe_{1-c}Cr_c$ alloys are listed in Table IV and compared to the experimental data[18] in Fig. 3. We find that theory slightly overestimates $B(c)$, $G(c)$, and $E(c)$. This overestimation, however, appears to be almost constant with c, which indicates that the errors obtained for pure Fe (Table II) are simply carried over to the random alloys. More importantly, the average experimental trends for $B(c)$, $G(c)$, $E(c)$, and $B/G(c)$ are very well captured by the present theory. In particular, the observed nonlinear behavior of $B(c)$ and $B/G(c)$ and the average positive slope of $G(c)$ and $E(c)$ are well reproduced by our results. The trends of polycrystalline elastic moduli are clearly connected to the trends obeyed by the equilibrium lattice parameter (Fig. 1) and single-crystal elastic constants (Fig. 2). For instance, the local minimum in $B(c)$ can partly be attributed to the volume expansion at low concentrations, whereas the positive slope of $E(c)$ and $G(c)$ is the consequence of the increasing $C_{44}(c)$ with Cr content.

In $Fe_{1-c}Cr_c$ solid solutions with $c \leq 0.2$, the largest alloying effects in $B(c)$ and $B/G(c)$ with respect to pure Fe are

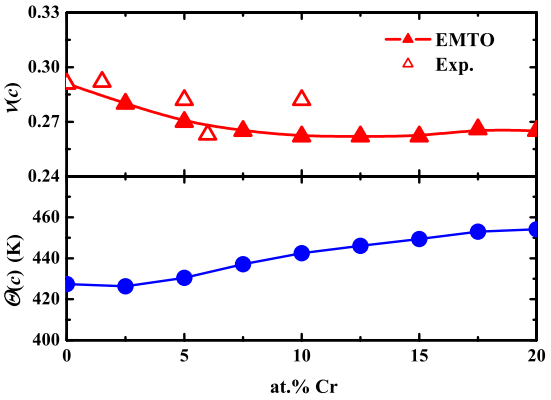

FIG. 4. (Color online) Theoretical (EMTO) and experimental (Ref. 18) Poisson's ratio (upper panel) and theoretical (EMTO) Debye temperature (lower panel) of ferromagnetic bcc $Fe_{1-c}Cr_c$ random alloys as a function of Cr concentration.

−8.3% (corresponding to $Fe_{0.95}Cr_{0.05}$) and −14.2% ($Fe_{0.875}Cr_{0.125}$), respectively. Furthermore, at 20 at. % Cr, $G(c)$ and $E(c)$ enhance by about 14.1% and 11.8%, respectively, relative to their values for pure Fe. According to the present $B/G(c)$, we find that small amount of Cr($c \lesssim 0.15$) makes the Fe-Cr alloy more brittle[62] compared to pure Fe. Nevertheless, placing the brittle-ductile boundary around $B/G \sim 1.75$,[35,62] most of the Fe-Cr solid solutions considered here remain far inside the ductile region.

The present Poisson ratio [$\nu(c)$] and the elastic Debye temperature [$\Theta(c)$] for Fe-Cr alloys are shown in Fig. 4 as a function of Cr content. The Poisson ratio slightly decreases with Cr concentration up to 10 at. % Cr, in line with the experimental data.[18] The Debye temperature has a local minimum at 2.5 at. % Cr, after which exhibits a monotonous enhancement with Cr content. In $Fe_{0.8}Cr_{0.2}$, the calculated Poisson ratio decreases by 8.9% and the Debye temperature enhances by 6.3% with respect to that for pure Fe.

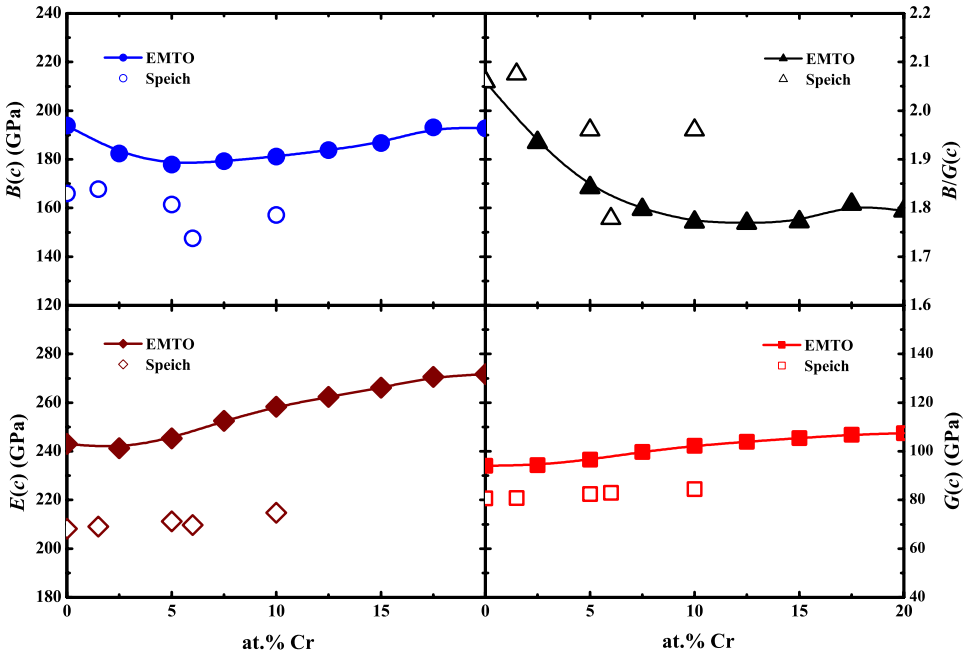

FIG. 3. (Color online) Theoretical (EMTO) and experimental (Speich) (Ref. 18) polycrystalline bulk modulus (B), Young's modulus (E), shear modulus (G), and B/G ratio for ferromagnetic bcc $Fe_{1-c}Cr_c$ random alloys as a function of Cr concentration.

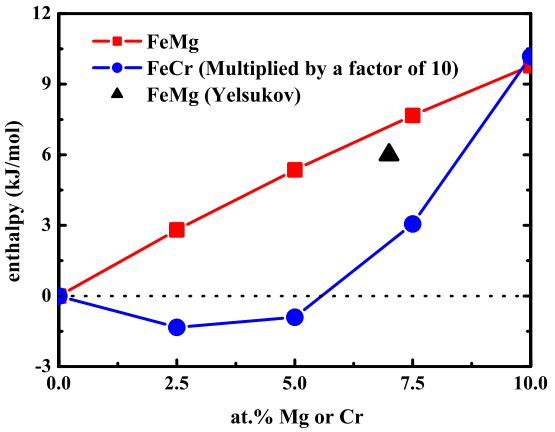

FIG. 5. (Color online) Theoretical (EMTO) enthalpy of formation for ferromagnetic bcc Fe-Mg random alloy. For comparison, the enthalpy of formation for Fe-Cr is also shown. The latter has been multiplied by 10 to match the scale. The predicted value by Yelsukov *et al.* (Ref. 7) for $Fe_{0.93}Mg_{0.07}$ is shown by triangle.

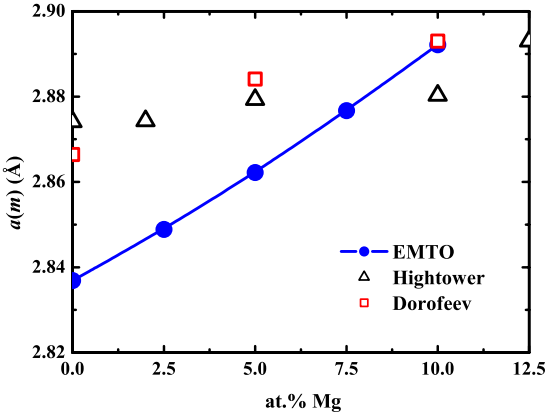

FIG. 6. (Color online) Theoretical (EMTO) lattice parameter of ferromagnetic bcc Fe-Mg random alloys as a function of Mg concentration. The experimental data are from Ref. 4 (Hightower) and Ref. 5 (Dorofeev).

From Figs. 1–4, we can see that the elastic properties of Fe-Cr alloys exhibit some anomalous behavior in the low Cr region. The local minima in $C_{11}(c)$, $C_{12}(c)$, and $B(c)$, and the corresponding discontinuities in the first-order derivatives of $G(c)$, $E(c)$, and $\Theta(c)$ around $c \approx 0.05$ suggest the presence of anomalous electronic transitions around this concentration. Recently, Korzhavyi *et al.*[63] reported a Fermi-surface topology change in the majority-spin channel in Fe-Cr alloys encompassing about 7 at. % Cr. We suggest that the disclosed anomalous trends of the elastic parameters from Figs. 1–4 are the manifestations of the above topological transition.

Based on our results obtained for Fe and Fe-Cr, we conclude that in general the EMTO method reproduces well the observed alloying effects in ferromagnetic bcc Fe-Cr alloys with Cr content up to 10 at. %. Therefore, we have confidence in this theoretical approach and use it to study the elastic properties of Fe-Mg random solid solutions for which no corresponding experimental data are available yet.

C. Elastic properties of Fe-Mg alloys

According to the experimental phase diagram, the solid solubility of Mg in Fe, and vice versa, is very small,[1] meaning that the formation energy of Fe-Mg alloy should be large and positive. In Fig. 5 we compare the formation enthalpy of Fe-Mg with that of Fe-Cr. For the standard states, we use the ferromagnetic bcc Fe, the antiferromagnetic B2 Cr, and the experimental hexagonal-close-packed (hcp) Mg with $c/a = 1.624$. The present enthalpy of formation for Fe-Cr shows a local negative minimum and becomes positive near 5.5% Cr, in good accordance with that reported in Refs. 28 and 63. The enthalpy of formation for Fe-Mg, on the other hand, is found to increase monotonously up to 10 kJ/mol obtained for $Fe_{0.90}Mg_{0.10}$. This result is in line with the predicted enthalpy of formation for Fe-Mg by de Boer *et al.*[64] and also with that calculated by Yelsukov *et al.*[7] for $Fe_{0.93}Mg_{0.07}$.

For the atomic radius of hcp Mg we obtained 1.764 Å, which agrees well with the experimental value of 1.77 Å.[55] Using this atomic radius and that of pure Fe(1.40 Å), for the bcc $Fe_{1-m}Mg_m$ alloys Vegard's rule predicts a lattice parameter with slope of $\Delta a(m)/\Delta m \sim 3.6 \times 10^{-3}$ Å per at. % Mg. The present EMTO results, shown in Fig. 6, give 5.5×10^{-3} Å increase per at. % Mg. Moderate lattice expansion upon Mg addition to Fe was also reported by Hightower *et al.*[4] and Dorofeev *et al.*[5] In their measurements, the average lattice expansion below $m=0.1$ was 0.6×10^{-3} and 2.7×10^{-3} Å per at. % Mg, respectively. Thus, similar to Fe-Cr, the present theoretical $\Delta a(m)/\Delta m$ seems to overestimate its experimental counterparts. On the other hand, the local experimental slope between 10 and 12.5 at. % Mg by Hightower *et al.* reaches 5.4×10^{-3} Å per at. % Mg, which is very close to the present value obtained for random solid solution. Surprisingly, our calculated density change of 11% obtained for $m=0.1$ is in perfect agreement with the average experimental value measured below 10 at. % Mg (Fig. 5 in Ref. 4).

In the following, we investigate the elastic properties of ferromagnetic bcc $Fe_{1-m}Mg_m$ $(0 \le m \le 0.1)$ random alloys as a function of Mg content. The present theoretical single-crystal elastic constants $C_{ij}(m)$ are listed in Table V and plotted in Fig. 7 as a function of Mg content. We find that all elastic constants decrease nearly linearly with Mg addition. The theoretical $C_{11}(m)$, $C_{12}(m)$, $C'(m)$, and $C_{44}(m)$ for $m=0.1$ change by about −36.3%, −34.2%, −38.2%, and −8.2%, respectively, compared to the corresponding values for pure Fe. The monotonously decreasing trends of the

TABLE V. Theoretical (EMTO) lattice parameters (in Å) and single-crystal elastic constants (in GPa) for the ferromagnetic bcc $Fe_{1-m}Mg_m$ $(0 \le m \le 0.1)$ random alloys.

m	$a(m)$	$C_{11}(m)$	$C_{12}(m)$	$C'(m)$	$C_{44}(m)$
0	2.8369	297.84	141.89	77.97	106.73
0.025	2.8489	263.70	125.25	69.22	103.62
0.05	2.8622	235.76	112.67	61.55	100.97
0.075	2.8767	210.97	102.41	54.28	98.903
0.10	2.8922	189.72	93.389	48.17	97.942

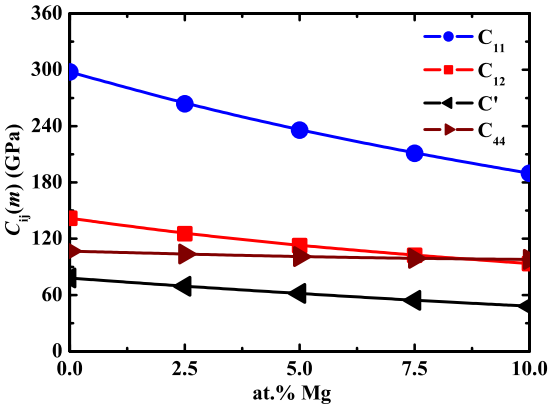

FIG. 7. (Color online) Theoretical (EMTO) single-crystal elastic properties of ferromagnetic bcc Fe-Mg random alloys as a function of Mg concentration.

single-crystal elastic constants of Fe-Mg (Fig. 7) are clearly different from those obtained for Fe-Cr (Fig. 2), indicating the absence of electronic topological transition in Fe-rich Fe-Mg random solid solutions.

Before turning to the polycrystalline elastic moduli, we discuss the effect of local lattice relaxation (LLR) around the impurity atoms on the single-crystal elastic constants. The LLR effect, neglected in the EMTO-CPA calculations, is expected to become important in systems with large volume mismatch. Here we use a supercell technique to establish the order of magnitude of the effect of LLR on the C' elastic constant of Fe-Mg and Fe-Cr solid solutions. The $2\times2\times2$ bcc supercell contained one Mg (or Cr) atom and 15 Fe atoms. First we calculated the tetragonal elastic constant of $Fe_{15}Mg_1$ ($Fe_{15}Cr_1$) using ideal bcc underlying lattice with lattice constant fixed to that obtained in a CPA calculation performed for the bcc $Fe_{0.9375}Mg_{0.0625}$ ($Fe_{0.9375}Cr_{0.0625}$) random alloy. Next we relaxed the first eight nearest-neighbor (NN) Fe atoms around the impurity atom and recalculated C' for the relaxed structure. In these calculations, we used ~2500 uniformly distributed k points in the irreducible wedge of the Brillouin zone. Results from the supercell calculations are summarized in Table VI. We find that in $Fe_{15}Mg_1$ the equilibrium Fe-Mg distance is ~0.8% larger than the equilibrium Fe-Fe bond length in pure bcc Fe. This figure may be contrasted with ~0.1% contraction of the Fe-Cr distance in the Fe-Cr system relative to the Fe-Fe bond length. Comparing the tetragonal elastic constant calculated for the supercell having the ideal bcc structure (C'_u) to that calculated for the supercell with relaxed Fe-impurity distance (C'_r), we can estimate the LLR effect in C'. In $Fe_{15}Mg_1$ this effect is ~0.7 GPa and in $Fe_{15}Cr_1$ ~0.2 GPa. Since the alloying effects for both systems are significantly larger than the above LLR effects (Tables III and V), we conclude that the composition dependence of the elastic parameters of Fe-Mg and Fe-Cr systems is well captured by the present EMTO-CPA approach.

TABLE VI. Results of the supercell calculations for $Fe_{15}Mg_1$ and $Fe_{15}Cr_1$ systems. δ_{NN} is the relaxation of the first-nearest neighbor Fe atoms around the impurity atom. C'_u and C'_r (in GPa) are the tetragonal elastic constants obtained for the supercells without and with local lattice relaxation, respectively.

System	C'_u	δ_{NN}	C'_r
$Fe_{15}Mg_1$	56.61	0.8%	57.33
$Fe_{15}Cr_1$	77.40	–0.1%	77.57

The theoretical polycrystalline elastic moduli for ferromagnetic bcc $Fe_{1-m}Mg_m$ ($0\leq m\leq0.1$) random alloys are displayed as a function of Mg content in Fig. 8 and Table VII. Similar to the single-crystal elastic constants (Fig. 7), the polycrystalline elastic moduli also decrease with Mg content. These results could in fact be anticipated if, for instance, we take into account that the theoretical bulk modulus of hcp Mg is significantly smaller than that of bcc Fe. However, the

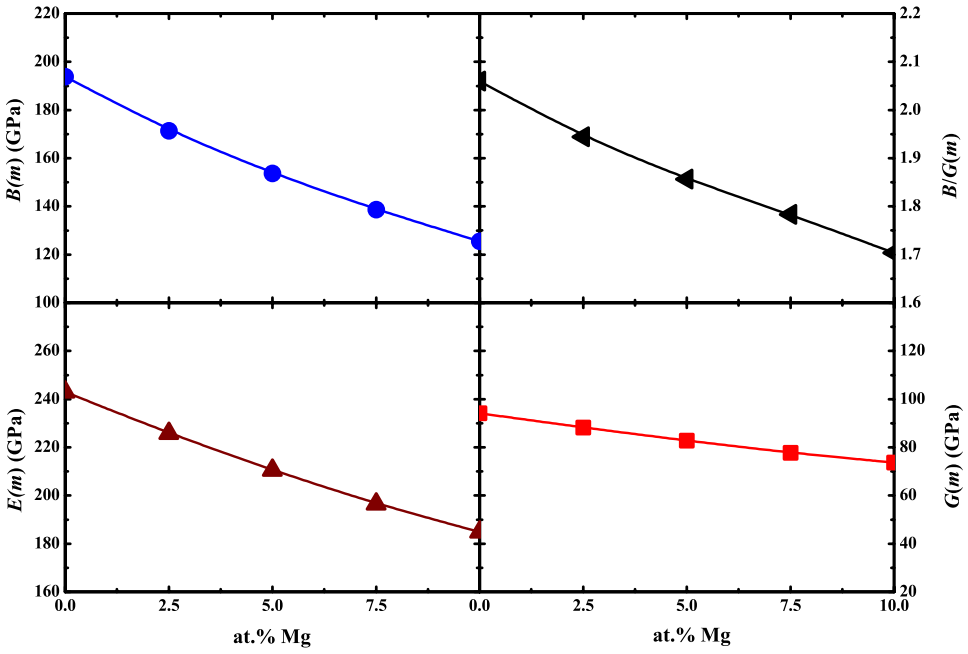

FIG. 8. (Color online) Theoretical (EMTO) polycrystalline elastic properties of ferromagnetic bcc $Fe_{1-m}Mg_m$ ($0\leq m\leq0.1$) random alloys as a function of Mg concentration.

TABLE VII. Theoretical (EMTO) polycrystalline elastic constants (in GPa), Poisson's ratio (ν), and Debye temperature (Θ, in K) for the ferromagnetic bcc $Fe_{1-m}Mg_m$ ($0 \leq m \leq 0.1$) random alloys.

m	$B(m)$	$G(m)$	$B/G(m)$	$E(m)$	$\nu(m)$	$\Theta(m)$
0	193.9	94.12	2.0598	243.03	0.291	427.41
0.025	171.4	88.15	1.9444	225.75	0.280	411.3
0.05	153.7	82.79	1.8565	210.56	0.272	396.34
0.075	138.6	77.74	1.7829	196.48	0.264	381.77
0.10	125.5	73.66	1.7038	184.83	0.255	369.24

actual slope of B in Fig. 8 is much larger than that predicted from the ~157 GPa difference between the theoretical bulk moduli of Fe and Mg by assuming a linear composition dependence for $B(m)$. We find that for $m=0.1$, $B(m)$, $G(m)$, $E(m)$, and $B/G(m)$ decrease by about 35.2%, 21.7%, 23.9%, and 17.3%, respectively, relative to those of pure Fe. Above 7.5 at. % Mg, the calculated $B/G(m)$ ratio of Fe-Mg alloys drops below the brittle-ductile limit of 1.75 set by Pugh,[62] implying that Mg addition makes the ferromagnetic bcc Fe-Mg alloys brittle.

The theoretical Poisson ratio and Debye temperature of Fe-Mg are shown in Fig. 9. Both of them exhibit a nearly linear decreasing dependence on the chemical composition. At 10 at. % Mg, the Poisson ratio and Debye temperature are by 12.4% and 13.6%, respectively, smaller than those corresponding to pure Fe. This Debye temperature drop when going from Fe to $Fe_{0.90}Mg_{0.1}$ is expected to give a phonon-vibration energy contribution which stabilizes the solid solution. To estimate this effect, we make use of the high-temperature expansion of the phonon energy.[65] Namely, for two solids with similar Debye temperatures, the vibrational free-energy difference is $\Delta F^{\mathrm{vib}} \approx 3k_B T(\Delta\Theta/\Theta)$, where T is the temperature, $\Delta\Theta/\Theta$ is the relative Debye temperature, and k_B the Boltzmann constant. We write the phonon free energy of formation for $Fe_{1-m}Mg_m$ as $\Delta F^{\mathrm{vib}}(m) = m[F^{\mathrm{vib}}(m) - F^{\mathrm{vib}}(\mathrm{Mg})] + (1-m)[F^{\mathrm{vib}}(m) - F^{\mathrm{vib}}(\mathrm{Fe})]$, where $F^{\mathrm{vib}}(m)$, $F^{\mathrm{vib}}(\mathrm{Mg})$, and $F^{\mathrm{vib}}(\mathrm{Fe})$ are the vibrational free energies for $Fe_{1-m}Mg_m$, Mg, and Fe, respectively. For $m=0.1$ we have $[\Theta(0.1) - \Theta(\mathrm{Fe})]/\Theta(\mathrm{Fe}) \approx -0.136$ and $[\Theta(0.1) - \Theta(\mathrm{Mg})]/\Theta(\mathrm{Fe}) \approx 0.129$, where for the Debye temperature of Mg we used 327 K.[48] Using these relative Debye temperatures, we arrive at $\Delta F^{\mathrm{vib}}(0.1) \approx -2.74 \times 10^{-3}\ T$ kJ/mol/K (referring to mole of atoms). For comparison, the configuration entropy for $Fe_{0.90}Mg_{0.1}$, evaluated within the mean-field approximations, is $\Delta F^{\mathrm{conf}}(0.1) \approx -2.70 \times 10^{-3}\ T$ kJ/mol/K. It is worth noting that according to Fig. 5, the total thermal free-energy $\Delta[F^{\mathrm{vib}}(0.1) + F^{\mathrm{conf}}(0.1)] = -5.44 \times 10^{-3}\ T$ kJ/mol/K would stabilize the random $Fe_{0.90}Mg_{0.1}$ solid solution at ~1840 K, i.e., slightly above the melting point of Fe.

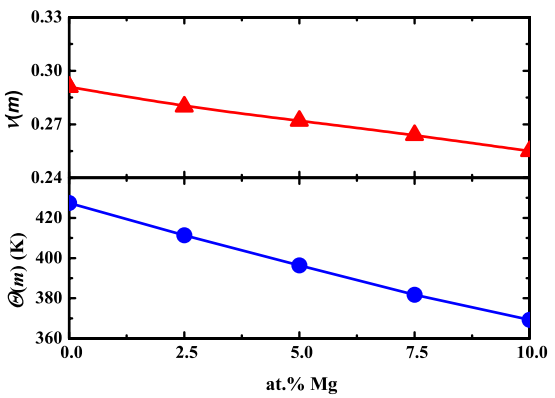

FIG. 9. (Color online) Theoretical (EMTO) Poison's ratio (upper panel) and Debye temperature (lower panel) of ferromagnetic bcc $Fe_{1-m}Mg_m$ ($0 \leq m \leq 0.1$) random alloys as a function of Mg concentration.

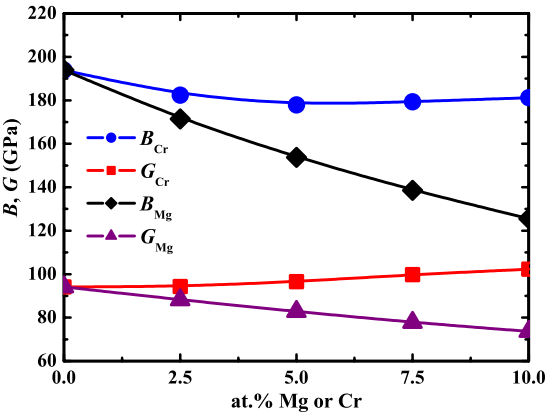

FIG. 10. (Color online) Comparison between the effect of Cr and Mg on the bulk and shear modulus of ferromagnetic bcc Fe-Cr and Fe-Mg random alloys calculated using the EMTO method.

Finally, for a direct comparison between the elastic properties of Fe-Cr and Fe-Mg alloys, in Fig. 10 we show the chemical composition dependence of the bulk modulus and shear modulus of the ferromagnetic bcc Fe-Cr and Fe-Mg random alloys for concentrations up to 10 at. % solute. Whereas the bulk modulus of Fe-Mg alloys reduces in a nearly linear manner, on the same scale the bulk modulus of Fe-Cr alloys shows a weak concentration dependence. The alloying effects on G upon Cr and Mg addition are totally different. In the Fe-Cr alloys, the shear modulus increases slowly with Cr amount. At the same time, G decreases significantly with increasing Mg concentration. We conclude that Mg addition reduces to a high degree the elastic moduli of Fe-Mg random alloys, while Cr has only a moderate impact on the elasticity of α-Fe.

IV. CONCLUSIONS

Using the EMTO method in combination with the coherent-potential approximation, we have calculated the single crystal and polycrystalline elastic properties of ferromagnetic bcc Fe-Cr random alloys encompassing up to 20 at. % Cr. The present theoretical polycrystalline data for Fe-Cr reproduce well the experimental trends[18] available below 10 at. % Cr, indicating that our theoretical tool is suitable to predict the elastic properties of Fe-based random solid solutions. Assuming a similar ferromagnetic bcc structure for Fe-Mg, we have investigated the effect of Mg addi-

tion on the elastic properties of Fe-rich Fe-Mg alloys.

In the Fe-Cr system, the lattice parameter and elastic properties exhibit anomalous composition dependence near 5 at. % Cr. We propose that these anomalies are due to the recently reported electronic topological transition in these alloys.[63] No similar peculiarities are seen in Fe-Mg alloys. For this system, all elastic parameters decrease in an almost linear manner with Mg addition. In general, Mg is found to have a more pronounced impact on the elastic properties of Fe-based alloys than that of Cr. In particular, the B/G ratio decreases by 17.3% when 10% Mg is added to bcc Fe, indicating that Mg reduces the ductility of Fe. According to the classical solid-solution strengthening models,[66,67] the large alloying effects obtained for the Fe-Mg alloys should result in an enhanced mechanical hardness. These predictions are subject for further theoretical investigations and call for well designed experimental studies on the mechanical properties of Fe-rich Fe-Mg solid solutions.

ACKNOWLEDGMENTS

The Swedish Research Council, the Swedish Foundation for Strategic Research, the Swedish Energy Agency, the China Scholarship Council, and the Hungarian Scientific Research Fund (Contract No. T048827) are acknowledged for financial support.

[1] *Binary Alloy Phase Diagrams*, edited by T. B. Massalsk (American Society for Metals, Metals Park, Ohio, 1986), Vol. 1.
[2] T. Haitani, Y. Tamura, T. Motegi, N. Kono, and H. Tamehiro, Mater. Sci. Forum **419-422**, 697 (2003).
[3] T. B. Massalski, in *Physical Metallurgy, Structure and Stability of Alloys*, edited by R. W. Cahn and P. Haasen (North-Holland, Amsterdam, 1996), Vol. 1, p. 134.
[4] A. Hightower, B. Fultz, and R. C. Bowman, Jr., J. Alloys Compd. **252**, 238 (1997).
[5] G. A. Dorofeev, E. P. Elsukov, and A. L. Ul'yanov, Inorg. Mater. **40**, 690 (2004).
[6] G. A. Dorofeev, E. P. Yelsukov, A. L. Ul'yanov, and G. N. Konygin, Mater. Sci. Forum. **343-346**, 585 (2000).
[7] E. P. Yelsukov, G. A. Dorofeev, and A. L. Ul'yanov, Czech. J. Phys. **55**, 913 (2005).
[8] N. Dubrovinskaia, L. Dubrovinsky, and C. McCammon, J. Phys.: Condens. Matter **16**, S1143 (2004).
[9] N. Dubrovinskaia, L. Dubrovinsky, I. Kantor, W. A. Crichton, V. Dmitriev, V. Prakapenka, G. Shen, L. Vitos, R. Ahuja, B. Johansson, and I. A. Abrikosov, Phys. Rev. Lett. **95**, 245502 (2005).
[10] O. K. Andersen, O. Jepsen, and G. Krier, in *Lectures on Methods of Electronic Structure Calculations*, edited by V. Kumar, O. K. Andersen, and A. Mookerjee (World Scientific, Singapore, 1994), p. 63.
[11] L. Vitos, H. L. Skriver, B. Johansson, and J. Kollár, Comput. Mater. Sci. **18**, 24 (2000).
[12] L. Vitos, Phys. Rev. B **64**, 014107 (2001).
[13] P. Soven, Phys. Rev. **156**, 809 (1967).
[14] B. L. Györffy, Phys. Rev. B **5**, 2382 (1972).
[15] L. Vitos, I. A. Abrikosov, and B. Johansson, Phys. Rev. Lett. **87**, 156401 (2001).
[16] L. Vitos, *Computational Quantum Mechanics for Materials Engineers* (Springer-Verlag, London, 2007).
[17] J. A. Rayne and B. S. Chandrasekhar, Phys. Rev. **122**, 1714 (1961).
[18] G. R. Speich, A. J. Schwoeble, and W. C. Leslie, Metall. Trans. **3**, 2031 (1972).
[19] G. Ghosh and G. B. Olson, Acta Mater. **50**, 2655 (2002).
[20] D. J. Dever, J. Appl. Phys. **43**, 3293 (1972).
[21] G. Y. Guo and H. H. Wang, Chin. J. Phys. (Taipei) **38**, 949 (2000).
[22] L. Vocadlo, G. A. de Wijs, G. Kresse, M. Gillan, and G. D. Price, Faraday Discuss. **106**, 205 (1997).
[23] K. J. Caspersen, A. Lew, M. Ortiz, and E. A. Carter, Phys. Rev. Lett. **93**, 115501 (2004).
[24] X. W. Sha and R. E. Cohen, Phys. Rev. B **74**, 214111 (2006).
[25] R. Hultgren, P. D. Desai, D. T. Hawkins, M. Gleiser, and K. K. Kelley, *Selected Values of the Thermodynamic Properties of Binary Alloys*, (American Society for Metals, Metals Park, Ohio, 1973), pp. 694–703.
[26] S. S. M. Tavaresa, R. F. de Noronha, M. R. da Silva, J. M. Neto, and S. Pairis, Mater. Res. **4**, 237 (2001).
[27] J. Cieslak, S. M. Dubiel, and B. Sepiol, J. Phys.: Condens. Matter **12**, 6709 (2000).
[28] P. Olsson, I. A. Abrikosov, L. Vitos, and J. Wallenius, J. Nucl. Mater. **321**, 84 (2003).
[29] P. Olsson, I. A. Abrikosov, and J. Wallenius, Phys. Rev. B **73**, 104416 (2006).
[30] P. Hohenberg and W. Kohn, Phys. Rev. **136**, B864 (1964).
[31] J. P. Perdew, K. Burke, and M. Ernzerhof, Phys. Rev. Lett. **77**, 3865 (1996).
[32] W. Kohn and L. J. Sham, Phys. Rev. **140**, A1133 (1965).
[33] J. Kollár, L. Vitos, and H. L. Skriver, in *Electronic Structure and Physical Properties of Solids: the Uses of the LMTO Method*, Lectures Notes in Physics, edited by H. Dreyssé (Springer-Verlag, Berlin, 2000), p. 85.
[34] O. K. Andersen, C. Arcangeli, R. W. Tank, T. Saha-Dasgupta, G. Krier, O. Jepsen, and I. Dasgupta, in *Tight-Binding Approach to Computational Materials Science*, edited by P. E. A. Turchi, A. Gonis, and L. Colombo, MRS Symposia Proceedings No. 491 (Materials Research Society, Pittsburgh, 1998), pp. 3–34.
[35] L. Vitos, P. A. Korzhavyi, and B. Johansson, Phys. Rev. Lett. **88**, 155501 (2002); Nature Mater. **2**, 25 (2003).
[36] L. Dubrovinsky, N. Dubrovinskaia, F. Langenhorst, D. Dobson, D. Rubie, C. Geβmann, I. A. Abrikosov, B. Johansson, V. I. Baykov, L. Vitos, T. Le Bihan, W. A. Crichton, V. Dmitriev, and H.-P Weber, Nature (London) **422**, 58 (2003).
[37] A. E. Kissavos, S. I. Simak, P. Olsson, L. Vitos, and I. A. Abrikosov, Comput. Mater. Sci. **35**, 1 (2006).
[38] L. Vitos, P. A. Korzhavyi, and B. Johansson, Phys. Rev. Lett. **96**, 117210 (2006).
[39] A. Taga, L. Vitos, B. Johansson, and G. Grimvall, Phys. Rev. B **71**, 014201 (2005).

[40] L. Huang, L. Vitos, S. K. Kwon, B. Johansson, and R. Ahuja, Phys. Rev. B **73**, 104203 (2006).
[41] J. Zander, R. Sandström, and L. Vitos, Comput. Mater. Sci. **41**, 86 (2007).
[42] B. Magyari-Köpe, G. Grimvall, and L. Vitos, Phys. Rev. B **66**, 064210 (2002).
[43] B. Magyari-Köpe, L. Vitos, and G. Grimvall, Phys. Rev. B **70**, 052102 (2004).
[44] B. Magyari-Köpe, L. Vitos, B. Johansson, and J. Kollár, Acta Crystallogr., Sect. B: Struct. Sci. **57**, 491 (2001).
[45] B. Magyari-Köpe, L. Vitos, B. Johansson, and J. Kollár, J. Geophys. Res. **107**, 2136 (2002).
[46] A. Landa, C.-C. Chang, P. N. Kumta, L. Vitos, and I. A. Abrikosov, Solid State Ionics **149**, 209 (2002).
[47] B. Magyari-Köpe, L. Vitos, G. Grimvall, B. Johansson, and J. Kollár, Phys. Rev. B **65**, 193107 (2002).
[48] G. Grimvall, *Thermophysical Properties of Materials* (North-Holland, Amsterdam, 1999).
[49] V. L. Moruzzi, J. F. Janak, and K. Schwarz, Phys. Rev. B **37**, 790 (1988).
[50] E. K. Delczeg-Czirjak, L. Delczeg, M. Ropo, K. Kokko, M. P. J. Punkkinen, B. Johansson, and L. Vitos, Phys. Rev. B **79**, 085107 (2009).
[51] R. Hill, Proc. Phys. Soc., London, Sect. A **65**, 349 (1952).
[52] P. A. Korzhavyi, A. V. Ruban, I. A. Abrikosov, and H. L. Skriver, Phys. Rev. B **51**, 5773 (1995).
[53] J. P. Perdew, J. A. Chevary, S. H. Vosko, K. A. Jackson, M. R. Pederson, D. J. Singh, and C. Fiolhais, Phys. Rev. B **46**, 6671 (1992).
[54] M. Ropo, K. Kokko, and L. Vitos, Phys. Rev. B **77**, 195445 (2008).
[55] D. A. Young, *Phase Diagrams of the Elements* (University of California Press, Berkeley, 1991).
[56] M. Aldén, H. L. Skriver, S. Mirbt, and B. Johansson, Surf. Sci. **315**, 157 (1994).
[57] R. Hafner, D. Spisak, R. Lorenz, and J. Hafner, Phys. Rev. B **65**, 184432 (2002).
[58] P. Söderlind, O. Eriksson, J. M. Wills, and A. M. Boring, Phys. Rev. B **48**, 5844 (1993).
[59] A. L. Sutton and W. Hume-Rothery, Philos. Mag. **46**, 1295 (1955).
[60] W. B. Pearson, *A Handbook of Lattice Spacings and Structures of Metals and Alloys* (Pergamon, Belfast, 1958), p. 532.
[61] P. Söderlind, R. Ahuja, O. Eriksson, J. M. Wills, and B. Johansson, Phys. Rev. B **50**, 5918 (1994).
[62] S. F. Pugh, Philos. Mag. **45**, 823 (1954).
[63] P. A. Korzhavyi, A. V. Ruban, J. Odqvist, J.-O. Nilsson, and B. Johansson, Phys. Rev. B **79**, 054202 (2009).
[64] F. R. de Boer, R. Boom, W. C. M. Mattens, A. R. Miedema, and A. K. Niessen, in *Cohesion in Metals: Transition Metal Alloys*, edited by F. R. de Boer and D. G. Pettifor (North-Holland, Amsterdam, 1988), Vol. 1.
[65] G. Grimvall, Phys. Scr. **13**, 59 (1976).
[66] L. Vitos and B. Johansson, in *Applied Parallel Computing: State of the Art in Scientific Computing*, Lecture Notes in Computer Science, edited by B. Kagström *et al.*, (Springer-Verlag, Berlin, 2007), Vol. 4699, p. 510.
[67] R. Labusch, Acta Metall. **20**, 917 (1972); R. L. Fleischer, *ibid.* **11**, 203 (1963); F. R. N. Nabarro, Philos. Mag. **35**, 613 (1977).